Intranuclear Filaments Containing a Nuclear Pore Complex Protein

Volker C. Cordes,* Sonja Reidenbach,* Andreas Köhler,* Nico Stuurman,‡ Roel van Driel,‡ and Werner W. Franke*

*Division of Cell Biology, German Cancer Research Center, D-69120 Heidelberg, Federal Republic of Germany; and ‡E.C. Slater Institute, University of Amsterdam, Amsterdam 1000 HD, The Netherlands

Abstract. Nuclear pore complexes (NPCs) are anchoring sites of intranuclear filaments of 3–6 nm diameter that are coaxially arranged on the perimeter of a cylinder and project into the nuclear interior for lengths varying in different kinds of cells. Using a specific monoclonal antibody we have found that a polypeptide of ~190 kD on SDS-PAGE, which appears to be identical to the recently described NPC protein "nup 153," is a general constituent of these intranuclear NPC-attached filaments in different types of cells from diverse species, including amphibian oocytes where these filaments are abundant and can be relatively long. We have further observed that during mitosis this filament protein transiently disassembles, resulting in a distinct soluble molecular entity of ~12.5 S, and then disperses over most of the cytoplasm. Similarly, the amphibian oocyte protein appears in a soluble form of ~16 S during meiotic metaphase and can be immunoprecipitated from egg cytoplasmic supernatants. We conclude that this NPC protein can assemble into a filamentous form at considerable distance from the nuclear envelope and discuss possible functions of these NPC-attached filaments, from a role as guidance structure involved in nucleocytoplasmic transport to a form of excess storage of NPC proteins in oocytes.

THE cytoplasm of eukaryotic cells contains diverse filamentous structures which are commonly subsumed under the collective term "cytoskeletal" filaments, including the actin-containing microfilaments, the myosin-containing thick filaments, the microtubules, and the intermediate-sized filaments (IFs).[1] The protein constituents of each of these filament categories have been characterized in great detail and formation by self-assembly has been demonstrated in vivo and in vitro for each of these filamentous systems.

By contrast, little is known about the various kinds of non-nucleoprotein filaments described in cell nuclei, with the exception of the nuclear lamins which belong to the IF protein family and which appear in association with the nuclear envelope, either as distinct filaments as in certain amphibian oocytes (for example see Scheer et al., 1976*a*; Aebi et al., 1986) or as densely woven webs (Fawcett 1966; Aaronson and Blobel, 1975; for reviews see Aebi et al., 1988; Forbes, 1992).

Filamentous structures observed within the confinements of the nuclear envelope can be classified into two broad categories: those that are common to the nucleus and the cytoplasm and those that are specific for the nucleus. As representatives of the first group, intranuclear microtubules occur as regular components of interphase or dividing intact nuclei in a variety of organisms, ranging from the macronuclei of ciliates to several forms of fungal mitoses (for examples see Franke and Reau, 1973; Kubai, 1975). Microfilaments of the actin-type have been noticed to form in the nucleoplasm under certain conditions (for example see Jockusch et al., 1974; Fukui and Katsumaru, 1979; Osborn and Weber, 1980), and recently even IFs have been shown to assemble within the nucleoplasm under specific conditions (Bader et al., 1991; Eckelt et al., 1992; Blessing et al., 1993).

As a representative of the nucleus-specific filaments, a characteristic type of intranuclear filaments of diameter 8–12 nm, containing a 145-kD protein, has been found in association with the nucleolar cortex and in the "medusoid bodies" derived therefrom (Franke et al., 1981; De la Espina et al., 1982; Krohne et al., 1982; Benavente et al., 1984). Fibrillar components have also been resolved within the various types of spheroid nuclear bodies (for review see Brasch and Ochs, 1992).

Particularly prominent are the nuclear pore complex (NPC)–associated, axial filaments of diameter 3–6 nm which extend from the inner annulus into the nucleoplasm for various lengths, in certain amphibian oocytes for up to 1 μm (Franke, 1970; Franke and Scheer, 1970*a*,*b*; for reviews see Franke, 1974; Maul, 1977; Kessel, 1983; Scheer et al., 1988; see also Jarnik and Aebi, 1991). These filaments,

Address all correspondence to Dr. Werner W. Franke, Division of Cell Biology, German Cancer Research Center, Im Neuenheimer Feld 280, D-69120 Heidelberg, FRG.

1. *Abbreviations used in this paper*: IF, intermediate filaments; NPC, nuclear pore complex.

which often appear to be arranged on the circumference of a hollow cylinder and often exhibit a beaded appearance, have so far been only described by EM. More recently a delicate NPC-proximal filamentous substructure has been identified and described as a fish trap-shaped array (also as "cages" or "baskets"; Ris, 1989, 1991; Jarnik and Aebi, 1991; Goldberg and Allen, 1992).

In particular in nuclei with a high pore complex frequency such as amphibian oocytes, the NPC-attached cylindrical arrays of filaments are abundant, projecting from the pore complex like tentacles from a jelly fish, and represent a major component of the nuclear cortex. Guided by a new mAb that specifically reacts with these NPC-attached filament tangles, we have identified a NPC protein as a general constituent of these filaments.

Materials and Methods

Isolation and Fractionation of Nuclei

Nuclear envelope-enriched fractions of murine liver were prepared (Krohne and Franke, 1983) with the following modifications. Liver of sacrificed mice were homogenized at 4°C in buffer A (2 mM $MgCl_2$, 70 mM KCl, 2 mM DTT, 30 μg/ml trypsin inhibitor) containing 0.44 M sucrose. After adjusting the homogenate to 2 M sucrose, nuclei were centrifuged over a 2.1 M sucrose-cushion (in buffer A) for 60 min in swinging buckets at 40,000 *g*. Sedimented nuclei were washed in buffer A with 0.44 M sucrose and were then either fractionated directly or frozen in liquid nitrogen and stored at −70°C, after resuspension in buffer A with 0.44 M sucrose and 20% glycerol. Numbers and concentrations of nuclei were determined by light microscopy using a Neubauer chamber.

Nuclei of culture cells were isolated as follows. Cells cultured on petri dishes were washed with 37°C PBS containing 2 mM EDTA and then homogenized in ice-cold PBS containing 2 mM EDTA, 0.5% Triton, 2 mM DTT, and 30 μg/ml trypsin inhibitor. Cells were centrifuged for 10 min at 1,000 *g* and 4°C. The sediment containing nuclei and other cytoskeletal elements was washed in PBS and then either further fractionated or frozen in liquid nitrogen and stored at −70°C. The supernatant was centrifuged at 4°C for 30 min at 200,000 *g*. The resulting high-speed supernatant was frozen and stored at −70°C or protein was precipitated with TCA.

Nuclear envelopes of *Xenopus laevis* and *Pleurodeles waltlii* oocytes isolated for immunolocalization experiments or gel electrophoresis were manually prepared as described (Krohne and Franke, 1983) with slight modifications. Nuclei were isolated in 83 mM KCl, 17 mM NaCl, 10 mM Tris-HCl, pH 7.2, and then washed twice in PBS with or without 2 mM $MgCl_2$. For immunolocalization experiments nuclei were subsequently perforated with a needle or torn into fragments with fine forceps to enhance antigen accessibility, and immediately incubated with antibodies (see below).

Production of mAbs

mAbs were prepared against nuclear matrix proteins as described (Stuurman et al., 1992). Their immunoglobulin subclasses were determined by using ELISA (subclass-specific antibodies from Medac, Hamburg, FRG) and peroxidase-coupled secondary antibodies (Sigma, München, FRG).

Gel Electrophoresis and Immunoblotting

Proteins were separated by SDS-PAGE (Laemmli, 1970; Thomas and Kornberg, 1975) and two-dimensional NEPHGE (O'Farrell et al., 1977). After transfer of proteins separated by gel electrophoresis to nitrocellulose (NC) membranes (see Cordes et al., 1991) these were blocked with 0.05% Tween 20 in PBS for 3–12 h and subsequently for 30 min with 1% BSA in PBS. Incubation of membranes with undiluted hybridoma cell culture supernatant was carried out for 3–5 h. Bound antibodies were detected by goat anti-mouse IgG coupled to alkaline phosphatase. After washing (see Cordes et al., 1991), the secondary antibodies were added and bound antibodies detected by color reaction (Promega, Heidelberg, FRG). Alternatively, the enhanced chemoluminescence (ECL) protocol of Amersham International (Amersham Buchler, Braunschweig, FRG) was used, in combination with the HRP-coupled secondary antibody of Promega. In this case NC membranes were blocked in TBS containing 0.05% Tween (TBST) with 5% milk powder for 1 h. Incubation of membranes with primary and secondary antibodies was likewise carried out in the presence of 5% milk powder. For control experiments mAb RL11, described to recognize a NPC protein of ~180 kD which is modified with O-linked *N*-acetylglucosamine monosaccharides (Snow et al., 1987; Holt et al., 1987; a kind gift of Dr. L. Gerace, Scripps Research Institute, La Jolla, CA) and rabbit antibodies against "nup 153" described by Sukegawa and Blobel (1993) were used (kindly provided by these authors).

Microscopy and Immunolocalization

In most localization experiments, undiluted PF190×7A8 hybridoma cell culture supernatants were used. mAb RL11 (Snow et al., 1987) and the rabbit antibodies against "nup 153" (Sukegawa and Blobel, 1993) were used for comparison. Immunofluorescence microscopy on tissue cryosections was essentially as described (for example see Jahn et al., 1987). For immunofluorescence studies of cell cultures, these were either fixed with methanol (−20°C, 5 min) and/or acetone (−20°C, 1 min) or with 2% formaldehyde freshly prepared from paraformaldehyde (in PBS, pH 7.4) for 10 or 15 min. After aldehyde fixation, cells were washed with PBS containing 0.5% Triton X-100 for 5 min, before incubation with antibodies.

For electron microscopic localization, cryosections were fixed in acetone (−20°C) for 5 min and subsequently air dried for 30 min. After incubation with antibodies (in this case, supernatants were concentrated 1:3 by ultrafiltration; see Cordes and Krohne, 1993), sections were washed three times for 2 min with PBS and incubated for 12–14 h with goat anti-mouse IgG + IgM (Amersham Buchler) coupled to colloidal gold particles of 5 or 10 nm diameter. Fixation and embedding procedures were as described (Kartenbeck et al., 1984; Cowin et al., 1986).

For immunoelectron microscopy on manually isolated nuclei or nuclear envelopes of *Xenopus laevis* and *Pleurodeles waltlii* oocytes (Krohne and Franke, 1983) these were incubated with antibodies for 4 h at 4°C, washed three times with PBS and incubated with 10-nm gold-conjugated goat anti-mouse IgG (Amersham) for 12–14 h at 4°C. Alternatively, nuclear envelopes or fragments thereof were fixed for 10 min in 2% formaldehyde, freshly made from paraformaldehyde in PBS, and collected by centrifugation (2 min at 13,000 *g*). The pellet was washed several times in PBS containing 50 mM NH_4Cl. After incubation of the resuspended envelopes with the primary antibodies for 1.5 h and washes in PBS they were incubated with the secondary, gold (5 or 10 nm large particles)-coupled antibodies for another 3 h and again washed with PBS. Further fixation with glutaraldehyde, dehydration, embedding, and sectioning was as described (for references see above). For conventional ultrathin section EM the isolated envelopes or fragments thereof were fixed with glutaraldehyde and processed essentially as described (for example see Krohne et al., 1978; Franke et al., 1981).

In some experiments oocyte nuclei were incubated, in parallel, in PBS containing either 1 mM $CaCl_2$ or 2 mM EGTA or 1 mM $MgCl_2$ for 15 min before antibody application.

Random or serial sections were used for distance measurements and quantitative evaluations of immunogold particle distributions, applying conventional histographic methods.

Cell Culture and Mitotic Arrest

Mouse 3T3-L1 cells (semi-confluent) were cultured in 10-cm petri dishes in 90% DME and 10% FCS. To arrest cells in M-phase, 10^{-5} M colcemid was added to the medium (37°C) and cells were harvested after 9–10 h of incubation. At this time, >90% of the cells had the spheroid appearance typical of mitotic cells (frequence of mitoses was repeatedly controlled by DNA- and immunostaining). Cells were washed once with PBS, 2 mM $MgCl_2$ of 37°C and were then lysed either by incubation in digitonin buffer (250 mM sucrose, 20 mM Tris-HCl, pH 7.4, 70 mM KCl, 2 mM $MgCl_2$, 1 mM EGTA, 1 mM DTT, 30 μg/ml trypsin inhibitor, containing 0.005% digitonin) for 5 min at room temperature or by incubation in hypotonic buffer (20 mM Tris-HCl, pH 7.4, 15 mM KCl, 2 mM $MgCl_2$, 2 mM DTT, 30 μg/ml trypsin inhibitor, 10 μg/ml leupeptin) for 30–40 min on ice. Swelling of cells was controlled by light microscopy. After vigorously shaking the cells for 10 s the suspension was centrifuged for 30 min in a TLA 100.2 rotor (Beckman, München, FRG) at 200,000 *g* at 4°C. The sediment was frozen in liquid nitrogen and stored at −70°C. The supernatant ("mitotic cell extract") was either directly fractionated by sucrose density gradient centrifugation or frozen until further analysis.

Sucrose Gradient Density Centrifugation

Density gradient analysis of soluble proteins was on 5–30% (wt/vol) sucrose gradients (Huegle et al., 1985) in 20 mM Tris-HCl, pH 7.4, 90 mM KCl, 10 mM NaCl, 2 mM $MgCl_2$, 2 mM DTT, 30 μg/ml trypsin inhibitor, 10 μg/ml leupeptin, 10 μg/ml pepstatin. 400–500 μl mitotic cell extract was loaded per gradient (total volume 13.5 ml). BSA, catalase, and thyroglobulin (Pharmacia, Freiburg, FRG) were used as S-value reference proteins in parallel gradients or after mixing with the mitotic extract sample. Centrifugation was for 17 h at 230,000 *g* and 4°C in swinging buckets, and gradients were fractionated at a flow rate of 1 ml/min. Fractions of 0.4 ml were collected and immediately supplemented with 1/10 volume of 100% TCA.

Proteins and particles contained in supernatant fractions from *Xenopus* egg extracts were similarly analysed. Egg extracts were prepared as described (Felix et al., 1989), but without activating the eggs. The egg extract supernatant obtained after 1 h centrifugation at 100,000 *g* and 4°C was loaded on 5–30% sucrose gradients in 100 mM K-acetate, 2.5 mM Mg-acetate, and 60 mM EGTA, pH 7.2. Centrifugation was carried out as described for mitotic extracts.

Immunoprecipitation of Xenopus p190

100 μl of 100,000 *g* egg extract supernatant was combined with 50 μl PBS-washed and pre-swollen protein G-Sepharose (Pharmacia) and 350 μl PBS, 0.1% Triton X-100. After 30 min of incubation by rotation at 4°C, the Sepharose was sedimented for 5 min at 800 *g* to remove nonspecifically absorbing material. The remaining supernatant was then added to a new aliquot of 50 μl pre-swollen and washed protein G-Sepharose and 100 μl of mAb PF190x7A8. (For this experiment the IgGs have been precipitated from hybridoma cell culture supernatants with 48% $[NH_4]_2SO_4$ and resuspended in 0.1 volume of PBS.) After incubation for 2 h at 4°C and centrifugation for 5 min at 800 *g* the sediment was washed four times with PBS, twice with PBS, 0.1% Triton and again with PBS. Subsequently the sediment was boiled in SDS-PAGE sample buffer (Laemmli, 1970) for 5 min and analyzed by SDS-PAGE. For control, the supernatant after the antibody incubation was treated with 10% TCA and the precipitate obtained was analyzed by SDS-PAGE.

Results

Specificity of Antibodies

Among a variety of murine mAbs obtained from mice immunized with total "nuclear matrix" residues from extracted rat liver nuclei (see Stuurman et al., 1992) we found an IgG1 mAb (PF190x7A8) which in immunoblot experiments specifically reacted with an ~190-kD polypeptide present in a wide range of murine tissues and cell culture lines (examples are shown in Fig. 1, *a* and *b*). During cell fractionation, most of the epitope-bearing polypeptide was recovered in the Triton X-100 residue (fig. 1 *b*, lanes *2* and *3*) and was also resistant to extractions with low ionic strength buffers and treatment with RNase and DNase (Fig. 1, *c* and *c'*, lanes *1–4*). Most of the antigen, however, could be extracted by brief incubation in buffers of moderately high salt (e.g., 1 M

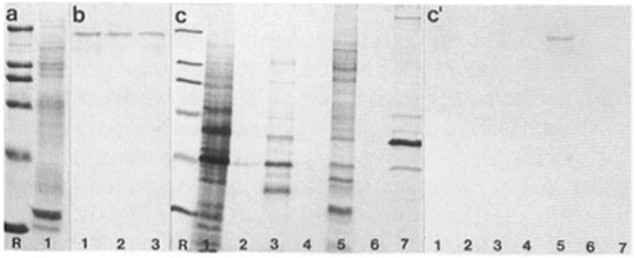

Figure 1. Immunoblot detection of the murine ~190-kD nuclear protein with mAB PF190x7A8. (*a*) Separation of total mouse liver nuclei by SDS-PAGE and staining with Coomassie blue (lane *1*); Relative masses of reference proteins (lane *R*) are, from top to bottom, as follows: 205, 116, 97, 66, 45, and 29 kD. (*b*) Immunoblot reaction (phosphatase) of total nuclear proteins from murine liver (lane *1*), Ag8 myeloma cells (lane *2*), and 3T3-L1 cells (lane *3*) with mAb PF190x7A8. (*c*) Fractionation of proteins from 3T3-L1 cells, separated by SDS-PAGE and stained with Coomassie blue. Lanes *1–6* represent the specific supernatants of the differential fractionation steps; lane *7* contains the resulting final pellet. PBS-0.5% Triton X-100 extraction (lane *1*), 10 mM Tris-HCl, pH 7.5, wash (lane *2*), DNase/RNase treatment (lane *3*), 10 mM Tris-HCl, pH 7.5, wash (lane *4*), first 1 M KCl extraction (lane *5*), second extraction with 1 M KCl (lane *6*). Reference proteins (lane *R*) as in *a*. (*c'*) Immunoblot of fractions shown in *c*, by reaction with mAb PF190x7A8.

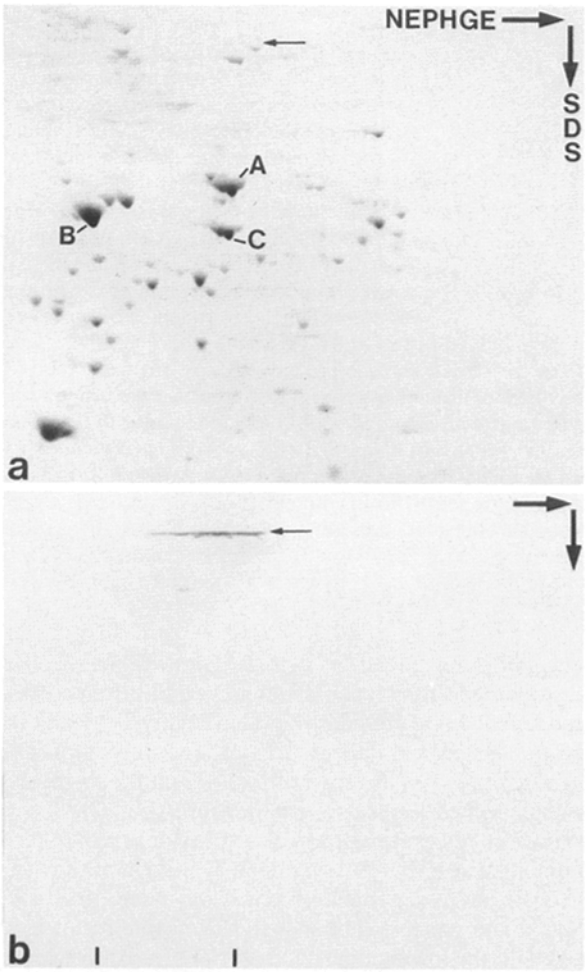

Figure 2. Characterization of the ~190-kD nuclear protein from mouse liver by two-dimensional gel electrophoresis. Proteins were separated by non-equilibrium pH gradient electrophoresis (*NEPHGE*) in the first and by SDS-PAGE in the second dimension (*SDS*). (*a*) Coomassie blue staining. Lamins A, B (representing lamin B1) and C and labeled. The small horizontal arrow denotes the position of the ~190-kD polypeptide (see below). (*b*) Immunoblot showing reaction with mAb PF190x7A8. Arrow denotes the ~190-kD protein, vertical bars indicate the positions of lamins B1 and A, respectively. Note the unusually heterogenous ("streaky") migration of the ~190-kD polypeptide under non-equilibrium conditions used. Whether this appearance, unexpected for a basic protein (see Sukegawa and Blobel 1993), is due to an intrinsic property of the polypeptide or to specific modifications remains to be examined.

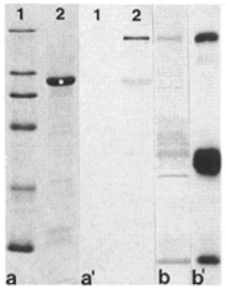

Figure 3. Immunoblot detection of the ~190-kD amphibian protein with mAb PF190x7A8. (*a*) Separation of manually isolated *Xenopus laevis* oocyte nuclear envelopes by SDS-PAGE, and staining with Coomassie blue (lane *2*); the white dot denotes the position of the inevitable contaminating major yolk protein. Reference proteins (lane *1*) are, from top to bottom: 205, 116, 97, 66, 45, and 29 kD. (*a'*) Immunoblot reaction (ECL procedure) of nuclear envelope proteins (same as in *a*) (lane *2*) with mAb PF190x7A8 on nitrocellulose filter. Lane *1* contains the same reference proteins as in *a*. (*b*) Separation of proteins obtained in immunoprecipitates from *Xenopus laevis* egg extract proteins with mAb PF190x7A8 after staining with Coomassie blue. (*b'*) Immunoblot reaction (ECL) of immunoprecipitated *Xenopus laevis* egg extract proteins with mAb PF190x7A8. The upper band contains the ~190-kD protein, the two lower bands represent heavy and light IgG chains.

KCl) concentration (Fig. 1, *c'*, lane *5*). On two-dimensional gel electrophoresis for 4 h and under non-equilibrium conditions the reactive polypeptides migrated relatively slowly in the first dimension and appeared in an unusually "streaky" fashion extending over a range of two pH-units, obviously not having reached isoelectric equilibrium. (Fig. 2).

When whole cell proteins or nuclear fractions from different mammalian species were examined by immunoblot reaction on SDS-PAGE separated proteins, the same ~190-kD band was found positive (not shown). The same result was obtained with the low amounts of material present in manually isolated nuclear envelopes from oocytes of the amphibian species, *Xenopus laevis* (Fig. 3, *a* and *a'*). In addition we found that this antibody was able to immunoprecipitate soluble protein material from *Xenopus* egg extracts which again, on SDS-PAGE and immunoblotting appeared as a positive ~190-kD band (Fig. 3, *b* and *b'*).

The ~190-kD polypeptide was recognized by mAbs RL1 and RL11 known to react with an O-glycosylated 180-kD rat NPC-attached protein (see Snow et al., 1987), and with rabbit antibodies specific for "nup 153" (Sukegawa and Blobel, 1993). With these antibodies positive immunoblot reactions with the ~190-kD protein were obtained on SDS-PAGE separated proteins of rodent liver nuclei and culture cells, and of immunoprecipitates from *Xenopus* egg extracts obtained with mAb PF190x7A8 (data not shown). We therefore and on the basis of immunolocalization criteria (see below), conclude that the antigen detected by mAb PF190x7A8 is immunologically related to, if not physically identical with "nup 153" (see also Discussion).

Under all conditions used the antibody did not cross react with other polypeptides of the O-glycosylated "nucleoporins" (Snow et al., 1987; see also Park et al., 1987; Davis and Blobel, 1987), the presence of which was routinely controlled by reaction with antibodies against p62 (see Cordes et al., 1991).

Immunolocalization in Somatic Cells

On monolayers of cultured cells, mAb PF190x7A8 exclusively immunostained nuclei in a finely punctate pattern (Fig. 4, *a–c*). This intense dot staining, which is typical of NPC proteins (for example see Davis and Blobel, 1986; Snow et al., 1987; Park et al., 1987; Radu et al., 1993; Sukegawa and Blobel, 1993), was observed in cells of a wide variety of species, including amphibia (Fig. 4, *a* and *a'*), rodents (Fig. 4 *b*), human (Fig. 4 *c*), and marsupials (see below). The appearance of small fluorescent dots and the negative reaction of nucleoli, chromosomes and other large intranuclear structures (e.g., Fig. 4, *a* and *a'*) was consistent with their occurrence in the nuclear periphery, i.e., with an NPC-association. Diminished immunofluorescence over intranuclear particles is also typical of other antibodies to NPC or nuclear lamina proteins (for example see Gerace et al., 1978, 1982; Krohne et al., 1978*a*; Burke et al., 1982; Snow et al., 1987).

A corresponding specific immunostaining of the nuclear periphery was also observed in cryosections of all tissues examined. Fig. 5 *a* presents mouse liver as an example.

When the distribution of the antigen was examined by immunoelectron microscopy, using 5-nm gold-coupled secondary antibodies, a specific decoration of NPC-associated structures was apparent (Fig. 5, *b* and *c*). Closer inspection further revealed that the majority of the immunogold particles were located on the inner, i.e., nuclear side of the pore complexes where they appeared to be associated with the NPC filamentous material extending into the nuclear interior (denoted by *arrows* in Fig. 5, *b* and *c*).

Immunolocalization in Amphibian Oocytes

Amphibian oocytes are particularly suitable objects for research of nuclear structures such as NPCs and their associated filaments, as extrachromosomal structures are dramatically amplified in the large nuclei ("germical vesicles") of vitellogenic oocytes (for NPC numbers and frequencies see Franke and Scheer, 1970*b*) and the NPC-attached filament arrays can often be traced for remarkable distances into the nuclear interior (see Franke and Scheer, 1970*a,b*, and below).

In frozen sections through amphibian ovaries, antibody mAb PF190x7A8 immunostained specifically the periphery of the oocyte nuclei of urodelan (Fig. 6 shows *Pleurodeles waltlii*) and anuran (e.g., *Xenopus laevis*, see below) species. This specific peripheral reaction was also seen when isolated unfixed nuclei or nuclear envelopes were examined by immunogold electron microscopy (Fig. 7 *a*). Clearly, pore complexes were decorated by the immunogold particles, however in a pronounced asymmetric distribution.

In all preparations, the outer and the inner aspect of the nuclear envelope could be easily identified, due to the retention of cytoplasmic organelles such as mitochondria, yolk platelets, and other vesicle membranes (e.g., Fig. 7 *b*) on the outer nuclear envelope aspect, vis-à-vis the occurrence of nucleolar structures on the other side of the envelope.

It is obvious from our immunoelectron microscopic results that the largest proportion of the antibodies was located at the loosely arranged bundles of 3–6-nm filaments projecting from the inner pore complex annulus for greatly varying distances. Corresponding to the variations of associated filamentous masses between different NPCs of the same envelope we also noted differences in the number of immunogold particles per NPC (e.g., Fig. 7, *a–f*). Some significant immunogold label was also seen in association

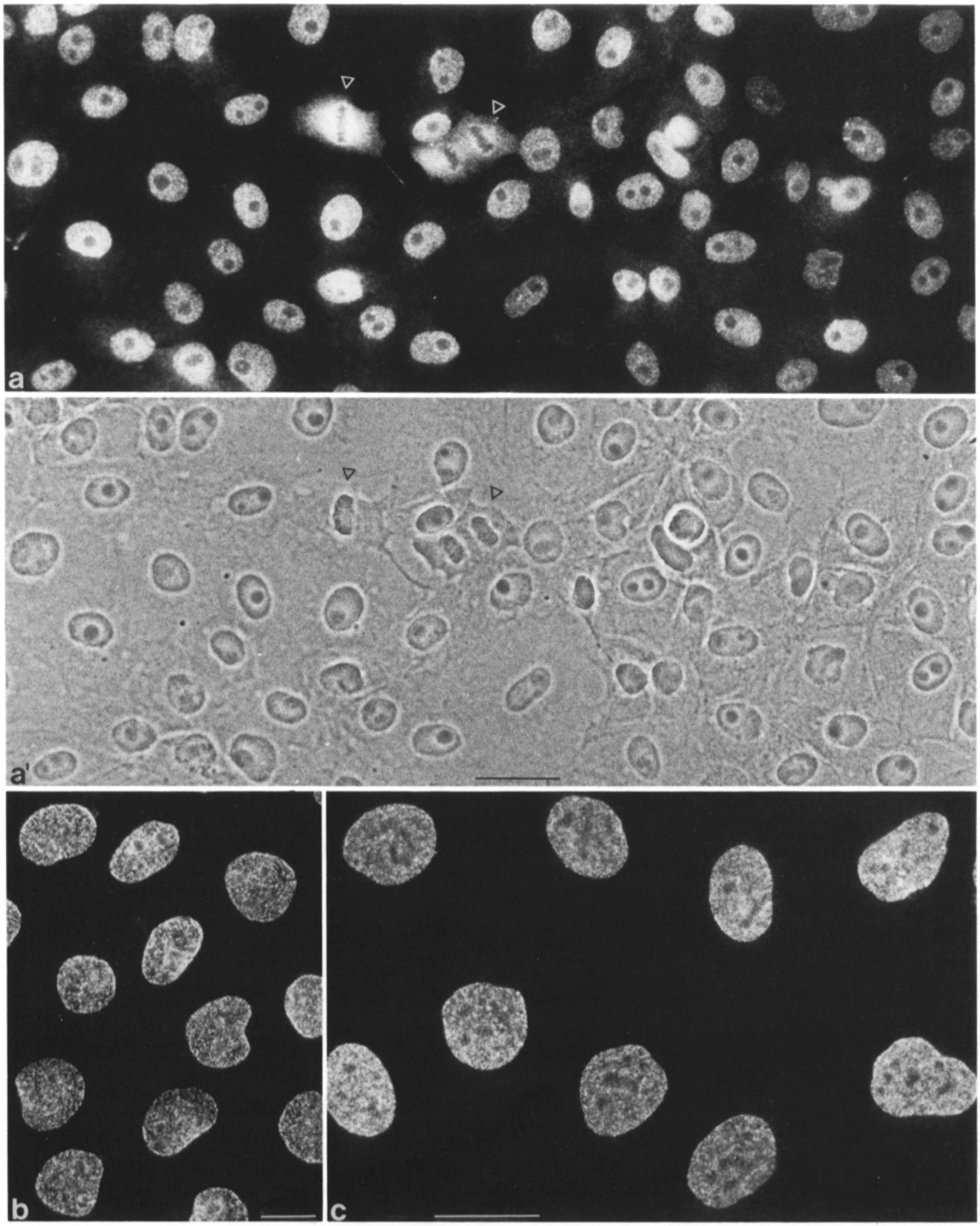

Figure 4. Immunofluorescence microscopy showing the location of the ~190-kD nuclear protein detected by mAb PF190x7A8 in cultured *Xenopus laevis* kidney epithelial cells of line A6 (*a* and *a'*); rat vascular smooth cells of line RV (see Franke et al., 1980) (*b*); and human liver carcinoma cells of line PLC (*c*). Cells were either fixed with methanol/acetone (*b* and *c*) or with formaldehyde, followed by incubation in PBS containing 0.5% Triton X-100 and incubation with the antibody (*a* and *a'*). (*a–c*) Epifluorescence optics, showing the specific nuclear location in a finely punctate pattern. (*a'*) Phase-contrast photograph corresponding to *a*. Arrowheads denote two mitotic cells. Bars: (*a*, *a'*, and *c*) 25 μm; (*b*) 20 μm.

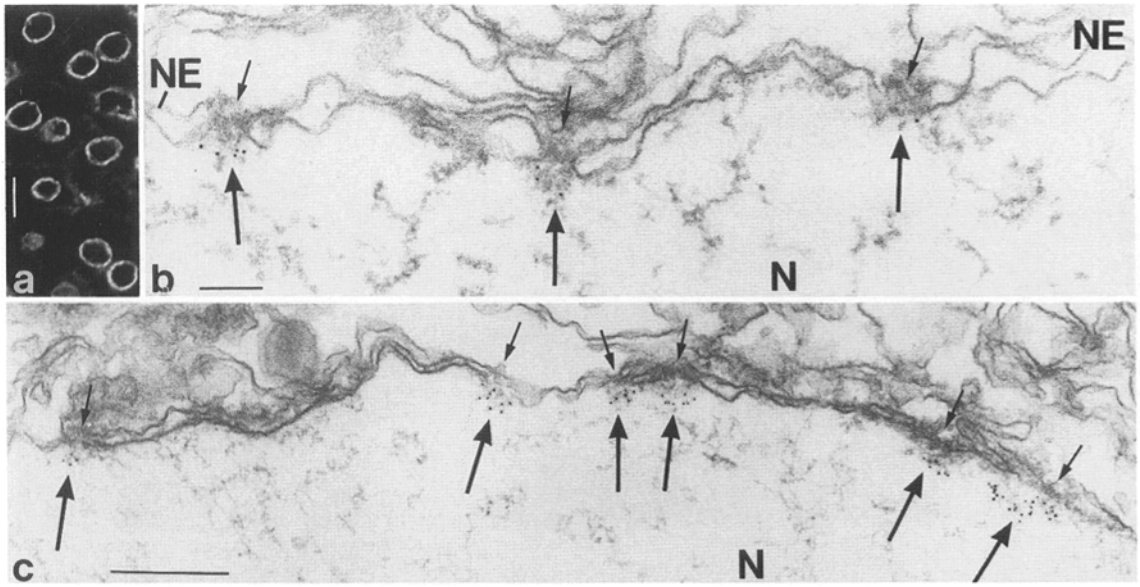

Figure 5. Immunolabeling of mouse liver cryosections with mAb PF190x7A8. (*a*) Immunofluorescence microscopy of tissue fixed with 2% formaldehyde, showing immunostaining in the nuclear periphery. (*b* and *c*) Electron microscopic immunogold localization (5-nm gold particles) on the intranuclear filamentous material (*thick arrows*) associated with the pore complexes (denoted by *thin arrows* on the cytoplasmic side). *NE*, nuclear envelope; *N*, nuclear interior. Cryosections were fixed with acetone. Bars: (*a*) 10 μm; (*b*) 0.1 μm; (*c*) 0.25 μm.

with the NPC proper and with its cytoplasmic aspect (e.g., Fig. 7, *a–c*). Occasionally encountered intranuclear annulate lamella cisternae also showed pore complex-associated filamentous material decorated with immunogold particles (Fig. 7 *f*).

Similar immunolocalization results as with mAb PF190x7A8 were obtained with mAb RL11 (fig. 8, *a* and *b*) and "nup 153" rabbit antibodies (Fig. 8, *c–e*). When determining the immunogold particle distribution between outer and inner side of the NPC for all three antibodies in different preparations the majority (72–93%) was found on the inner aspect of the NPCs with the attached filament bundles.

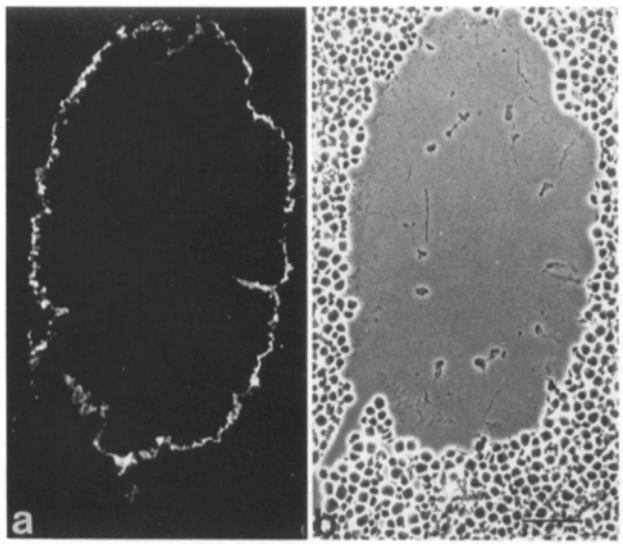

Figure 6. Immunofluorescence microscopy of an acetone-fixed cryosection through an amphibian oocyte (germinal vesicle-containing region of *Pleurodeles waltlii*) after reaction with mAb PF190x7A8. (*a*) Epifluorescence, showing specific reaction at the nuclear envelope. (*b*) Corresponding phase contrast photograph. Bar, 50 μm.

In such preparations the distribution of immunogold particles relative to the nuclear membrane and the NPC was also histographically determined. When the distance of each intranuclear immunogold grain from the corresponding NPC center level was measured, all three antibodies gave values falling into a similar distribution curve with 50–55 nm mean distance of all grains and maximal distances varying in different preparations from 140 to 330 nm.

The variations of filamentous masses attached to different NPCs indicated their lability during the preparation. Clearly the filamentous tufts retained on the inner NPC annulus of isolated and washed, unfixed nuclear envelopes were much shorter and less dense than those usually seen upon adequate fixation of intact oocytes (for example see Franke and Scheer, 1970*a*,*b*). As a special Ca^{2+}-dependence of NPC-attached filaments has recently been claimed (for example see Jarnik and Aebi, 1991; for review see Forbes, 1992) we systematically varied the divalent cation concentration of the buffers used for isolation of nuclei and nuclear envelopes (see Materials and Methods). The results obtained, however, did not show a significant effect of Ca^{2+} alone on filament preservation, and immunoreactive material was also found in nuclear envelopes treated with EGTA. To find a better compromise between structural preservation of the NPC-attached filaments on one hand and immunoreactivity and antigen accessibility on the other we included a brief aldehyde fixation step (see Materials and Methods). Fig. 9 *a* shows the resulting improved preservation of the nuclear filament cylinders associated with NPCs of isolated nuclear envelopes. These fixed filamentous arrays could still be traced for up to ~600 nm (see Fig. 9 *c*) and appeared very

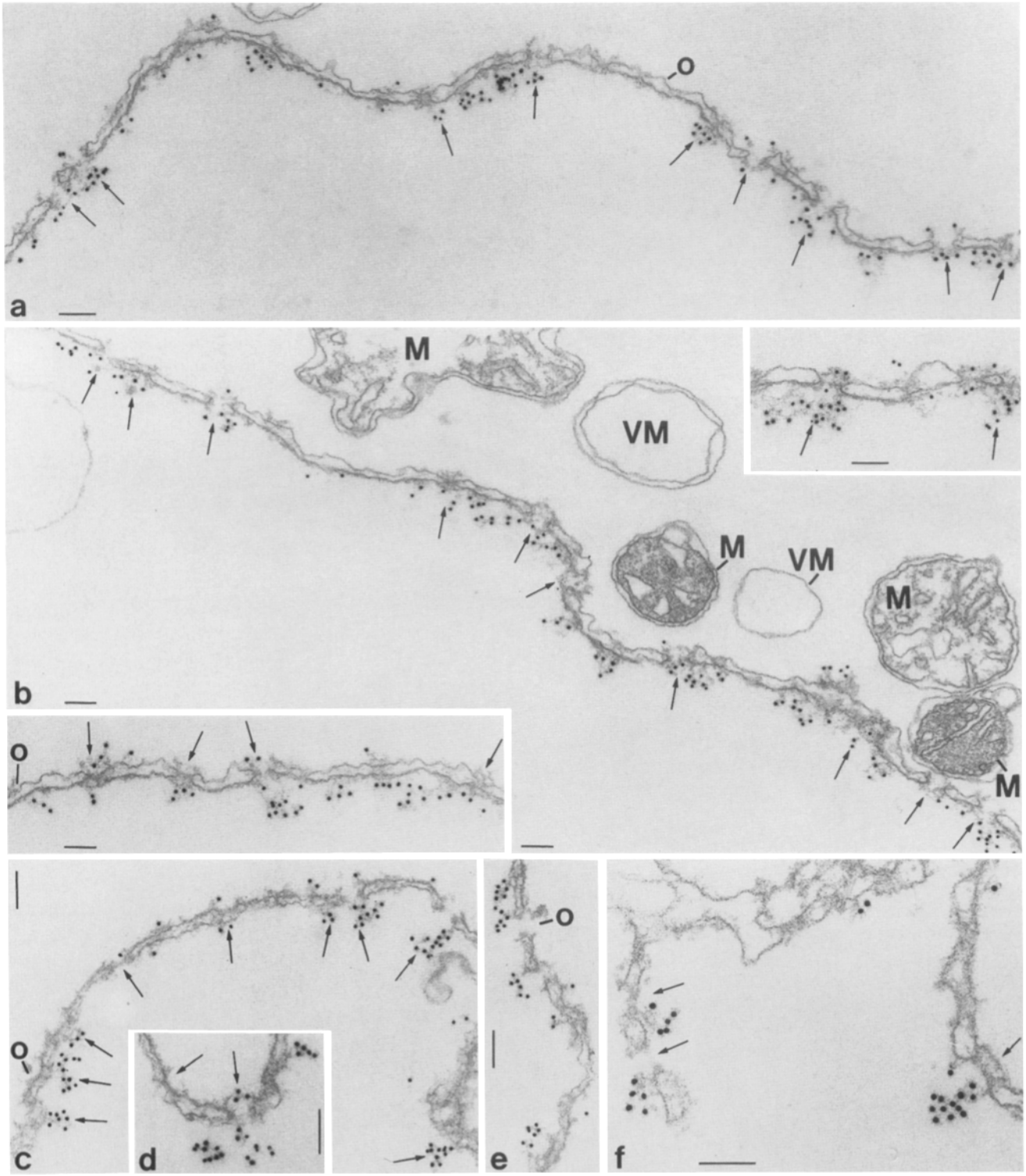

Figure 7. Immunoelectron microscopy of *Xenopus laevis* (*a* and *b*) and *Pleurodeles waltlii* oocytes (*c–f*) after reaction with mAb PF190x7A8. Immunogold localization (10-nm gold) on manually isolated and perforated nuclei (*o*, outer nuclear membrane) reveals intense decoration of nuclear pore complexes and NPC-associated filaments. (*a*) Survey micrograph showing association of the majority of the immunogold particles with the inner aspect of the nuclear envelope, particularly with the intranuclear filaments attached to NPCs (*arrows*). (*b*) Similar survey to that of *a* but showing, in addition, the adherence of cytoplasmic vesicles, vesiculated membranes (*VM*) and mitochondria (*M*) with the outer nuclear membrane. Insets show immunogold labeling at the inner NPC annulus and at filament tufts attached to the inner NPC annulus (*upper right inset*) but also, though lesser, at the outer NPC annulus (see some of the NPCs denoted by *arrows* in the *lower left inset*). (*c–e*) Details of intensely immunogold-labelled NPCs and NPC-attached intranuclear filament arrays (*o*, outer nuclear membrane). (*f*) Region showing immunogold decoration of filament bundles attached to inner annulus of an NPC of the nuclear envelope (*arrow* in the right) and both annuli of NPCs of intranuclear annulate lamellae (*arrows* in the left). Bars, 0.1 μm.

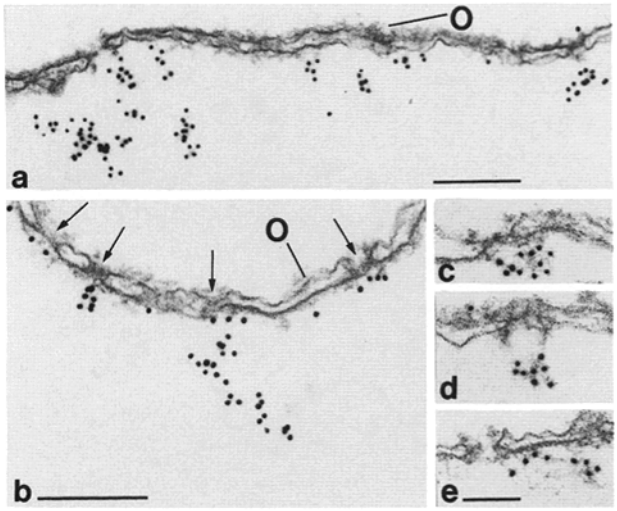

electron dense, were sometimes laterally entangled (see Fig. 9 *b*) and revealed a suborganization of thin (3–6 nm) flexible threads and associated granular structures of diameters up to 15 nm (e.g., Fig. 9 *c*).

Although the immunoreactivity of the PF190x7A8 antigen was considerably reduced upon this prefixation the residual immunolocalization clearly displayed a predominant association with the NPC-attached nuclear filament bundles, including sites distant from the nuclear envelope (Fig. 9 *d*). This immunogold labeling was also seen on the filamentous tangles extending between the NPCs and the cortices of

Figure 8. Immunoelectron microscopy of nuclear envelopes from *Xenopus laevis* oocytes after reaction with (*a* and *b*) mAb RL11 and (*c–e*) rabbit anti-nup153. Arrows in *b* denote nuclear pore complexes. *o*, outer nuclear membrane. Bars: (*a*) 0.25 μm; (*b*) 0.2 μm; (*c–e*) 0.1 μm.

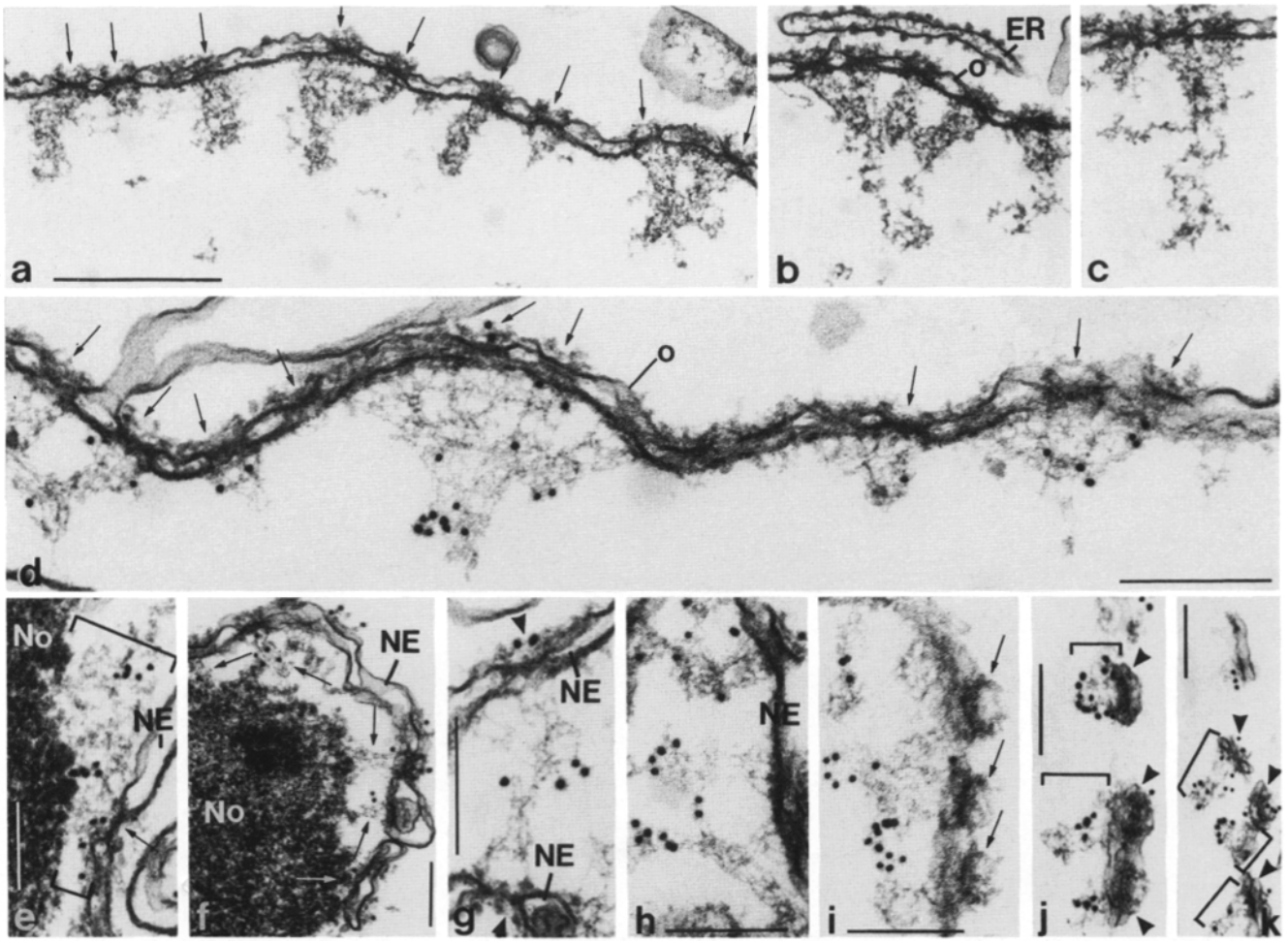

Figure 9. Electron micrographs showing the preservation of NPC-attached intranuclear filament cylinders in isolated envelopes from *Xenopus laevis* oocytes when fixed in formaldehyde (*a–c*) and then used for immunolocalization (*d–k*). (*a*) Survey micrograph showing the filamentous masses projecting from the inner annuli of the NPCs (*arrows*). Note that the cylinder arrays of NPC-attached filaments are mostly longer and more electron dense than those shown in Fig. 7. (*b*) After such fixation adjacent bundles of NPC-attached filaments often appear laterally aggregated and partly entangled. *ER*, endoplasmic reticulum cisterna. *o*, outer nuclear membrane. (*c*) Some NPC-attached filament bundles appear somewhat loosened, revealing substructural components. (*d*) Survey micrograph showing aldehyde fixation-stabilized nuclear envelopes after immunogold reaction with antibody mAb PF190x7A8 (symbols as in *a* and *b*). Note immunogold decoration of intranuclear filament bundles. *o*, outer nuclear membrane. (*e* and *f*) Immunogold labeling of filament tangles (demarcated by *brackets* in *e* and *arrows* in *f*) connecting NPCs with the cortex of adjacent nucleoli (*No*). *NE*, nuclear envelope. (*g*) Immunogold decoration of NPC-attached filaments sandwiched in a fold of the nuclear envelope (*NE*). Note that here the filament bundles of two opposite NPCs (*arrowhead*) are entangled into one unit. (*h* and *i*) Immunogold label on nuclear filament bundles attached to the residual NPCs (denoted by arrows in *i*) in regions in which most of the envelope membrane has been lost during the preparation. (*j* and *k*) Immunogold labeling of filament bundles (demarcated by brackets) retained on small nuclear envelope fragments containing one or two NPCs (*arrowheads*). Bars: (*a–c*) 0.5 μm; (*d*) 0.25 μm; (*e–k*) 0.2 μm.

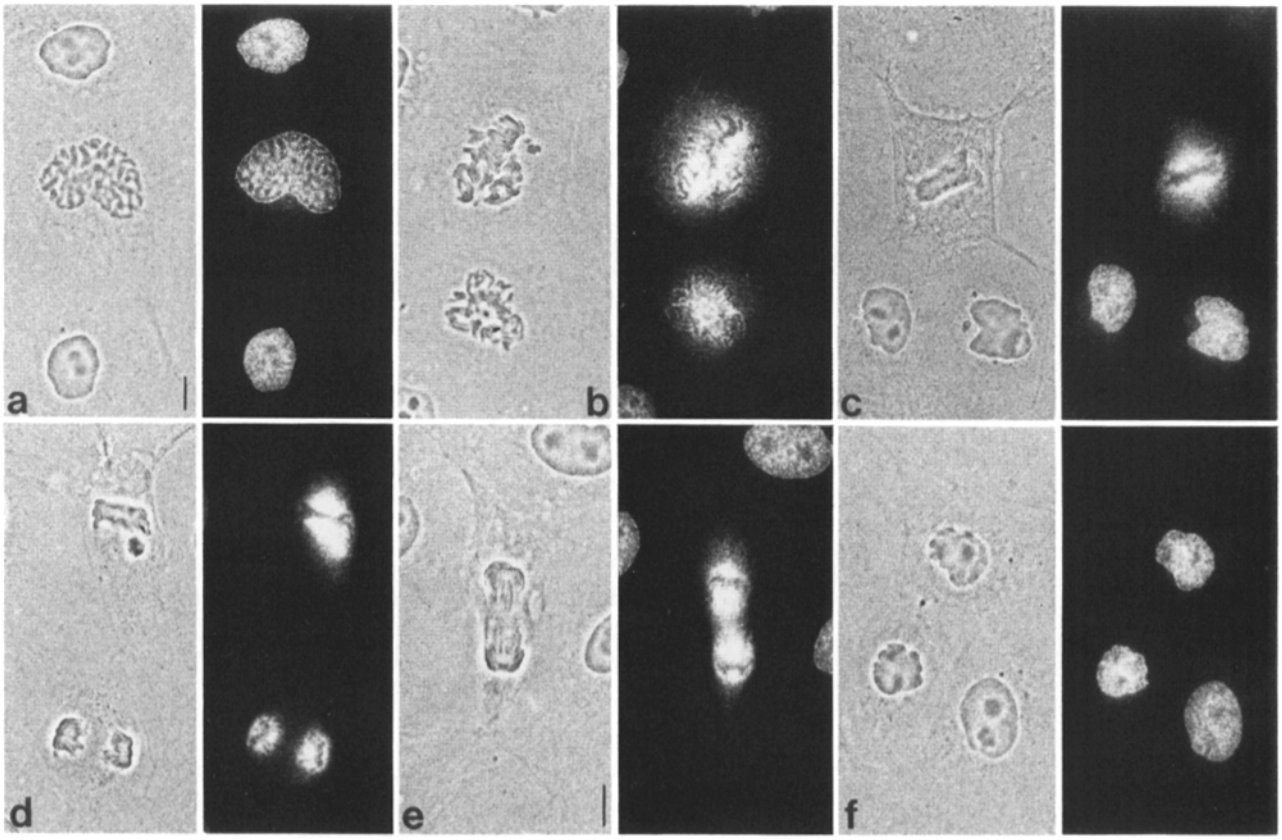

Figure 10. Immunofluorescence microscopy of the ~190-kD protein with mAb PF190x7A8 during mitosis of rat kangaroo kidney epithelial cells of line PtK2. Corresponding phase contrast and fluorescence micrographs showing different stages of mitosis: (*a*) Prophase, (*b*) Prometaphase, (*c*) Metaphase, (*d*) Anaphase (*top*) and telophase (*bottom*), (*e*) Telophase, and (*f*) Early G1 interphase. Bars, 10 μm.

nucleoli (Fig. 9, *e* and *f*) which are characteristically peripheral in this stage of oogenesis (for example see Scheer et al., 1976; Trendelenburg and McKinnell, 1979). The filamentous "bridges" between nucleoli and NPCs were particularly well discernible in situations in which the nucleoli were slightly more distant from the nuclear envelope (Fig. 9 *f*).

Isolated nuclear envelopes of the oocyte germical vesicles tend to fold in multiple ways (for example see Krohne et al., 1978*b*) so that "sandwiches" are formed in which the collapsed nuclear envelope regions include the entangled filament bundles of opposite NPCs (see Fig. 9 *g*). The aldehyde-fixed NPC-attached filaments were also preserved in nuclear envelope regions where large parts of the nuclear membrane structure had been lost (Fig. 9, *h* and *i*).

Occasionally, in some preparations including a prefixation step, small nuclear envelope fragments were seen which comprise only one or a few NPCs. It is notable that even such detached NPCs still reveal nuclear filament material positively labeled with the antibody (Fig. 9, *j* and *k*).

Disassembly of the 190-kD Pore Complex Filament Protein During Mitosis

The antigen recognized by mAb PF190x7A8 displayed markedly and characteristic changes of distribution during mitosis. Fig. 10, *a–f* presents the various mitotic stages in rat kangaroo kidney epithelial cells of line PtK2: At prophase-prometaphase transition the protein is still retained in the inner chromosomal phase, however, within the contours of the disintegrating nuclear envelope (Fig. 10 *a*). Subsequently, in metaphase and anaphase stages (Fig. 10, *b–d*), the protein disperses over the cytoplasm. The chromosomes are negative for this antigen. In telophase, the protein is reconcentrated around the chromosomal masses in the forming daughter nuclei (Fig. 10, *d* and *e*). Finally, early G1 nuclei again reveal the typical punctate pattern (Fig. 10 *f*).

This change from a state bound to a distinct structure to a more disperse form suggested a disintegration of the interphase filaments to smaller entities. This was corroborated by our fractionation results. In mitotically arrested cells most of the protein was recovered in the 200,000 *g* supernatant fraction (Fig. 11, *a* and *a'*). When the solubilized mitotic form was analyzed by sucrose gradient centrifugation (Fig. 11 *b*), the protein was detected in an almost monodisperse form with a peak sedimentation value of 12.5 S, indicative of a monomeric or small oligomeric state.

A distinct soluble form of the protein was also found in meiotic metaphase as determined in extracts from *Xenopus laevis* eggs. In such eggs the vast majority of the antigen was recovered in the 100,000 *g* supernatant fraction from which it could be immunoprecipitated (Fig. 3 *b* and *b'*), without coprecipitation of O-glycosylated NPC-protein p62, the other NPC protein so far characterized in this species (Dabauvalle et al., 1988; Cordes et al., 1991; see also

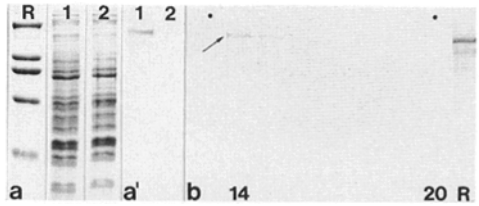

Figure 11. Gel electrophoretic analysis of the ~190-kD protein detected by mAb PF190x7A8 in fractions of soluble proteins from mitotically arrested murine 3T3-L1 cells. Cells were lysed either by incubation in iso-osmotic buffer containing 0.005% digitonin (*a* and *a'*) or hypotonically (*b*). Proteins were separated by SDS-PAGE and visualized by staining with Coomassie blue (*a*) or by immunoblotting with mAb PF190x7A8 (*a'* and *b*, phosphatase reaction). (*a*) Lane *R*, relative molecular masses of reference proteins in kD: 205, 116, 97, 66, 45, 29; (lane *1*) supernatant proteins from mitotic cells; (lane *2*) supernatant proteins from interphase cells. (*a'*) Corresponding immunoblots, showing the recovery of most of the ~190-kD protein in the supernatant fraction from mitotic cells (lane *1*) but not from interphase cells (lane *2*). (*b*) Immunoblot reaction showing the result of the analysis of the ~190-kD protein by sucrose gradient fractionation of proteins present in the 200,000 *g* supernatant fraction from mitotically arrested 3T3-L1 cells. Only fractions 13–20 obtained after sucrose gradient centrifugation are presented. The ~190-kD protein is detected in a peak-like distribution in fractions 14 and 15, corresponding to a mean S-value of 12.5. Peak positions of catalase (11.3 S) in fraction 13 and thyroglobulin (16.5 S) in fraction 20 are denoted by black dots. Mouse liver nuclear proteins were used in the same gel as reference (*R*).

Dabauvalle et al., 1990). The ~190-kD protein as present in egg extracts was also retained on WGA–Sepharose columns, in this case, however, together with p62 (not shown). When the soluble state of the ~190-kD protein was further analyzed by sucrose gradient centrifugation, a near monodisperse distribution with a mean peak value corresponding to ~16 S was found (data not shown).

Discussion

Our finding that a protein of the NPC also occurs as an apparently ubiquitous constituent of a specific kind of intranuclear NPC-attached filaments of diameter 3–6 nm not only provides the first compositional information on these nuclear structures but also shows that a NPC protein can assemble into a non-NPC structure and that this assembly does not require direct molecular contact with the nuclear membrane. In addition, our results demonstrate that these intranuclear NPC-attached filaments undergo a systematic disassembly–reassembly cycle during mitosis and meiosis.

As the polypeptide identified by mAb PF190x7A8 also specifically reacts with antibodies against protein "nup 153" recently sequenced and localized to the inner NPC annulus (Sukegawa and Blobel, 1993) and with mAb RL11, known to be specific for the same protein (Gerace, L., personal communication), we conclude that the protein localized in our study is "nup 153" or at least very closely related to it. Indeed, Sukegawa and Blobel (1993) have discussed the possibility, but did not show, that "nup 153" may also occur in the inner annulus-associated filamentous "cage" structure (Ris 1989, 1990; Jarnik and Aebi, 1991; Goldberg and Allen, 1992). At present we cannot distinguish between a localization in this "cage" and the other, partly longer filaments attached to the NPC although our findings of immunogold particles at distances clearly exceeding 60 nm indicates an occurrence beyond the confinements of this cage.

Our demonstration that the "nup 153"-like protein is a general component of NPC-attached filaments means that the number of molecules per NPC unit, i.e., NPC plus its attached cylindrical unit of filaments (see Franke and Scheer, 1970*a*,*b*), can by far exceed the eight copies estimated by Sukegawa and Blobel (1993). As in electron microscopic studies the length and mass density of the NPC-attached filament tangles vary considerably between different kinds of cells, the total amount of the filament-bound protein may also greatly vary. The observation that in amphibian oocytes these cylinders of coaxial filaments are conspicuously long and impressive (for example see Franke and Scheer, 1970*a*,*b*; Scheer et al., 1988) could be due to the special accumulation of this—and perhaps also other—NPC-associated proteins in filamentous assemblies, a form of stockpile similar to other maternal storages characteristic of this cell type (for review see Davidson, 1986). At present, we cannot decide whether and which other proteins may coassemble with the ~190-kD antigen described here to form these filament arrays at NPCs.

Our immunoelectron microscopic results show that the vast majority of these protein molecules is present in the intranuclear filaments attached to NPCs, although some significant immunogold label is also seen at the outer annulus. This localization in the intranuclear filaments distinguishes the "nup 153"-like protein from other NPC components reported to occur in the NPC proper, either on both annuli or at the NPC equator (Snow et al., 1987; for p62, see Davis and Blobel, 1986; Dabauvalle et al., 1988; for p155, see Radu et al., 1993; for p190 alias p210, see Gerace et al., 1982; for yeast nspl, see Nehrbass et al., 1990). Using the broadly reactive lectin WGA and an antibody (mAb RL1) cross-reactive with several different NPC proteins, Allen (1990) has shown immunolabeling of "fibrous material" on both sides of NPCs of rat liver cells (see also Park et al., 1987) but without identification of a specific molecule in one of these structures. By contrast, human polymyositis autoimmune sera that react, inter alia, with an ~180-kD polypeptide have specifically decorated filamentous tufts projecting from the outer annulus into the cytoplasm (Wilkin et al., 1993).

The exclusive localization of the RL11 antigen to the inner NPC annulus published by Snow et al. (1987) seems, at first sight, to be at variance with our localization of the RL11-reactive "nup 153"-like protein in the NPC-attached nuclear filaments. The specific experimental protocol of these authors, however, seems to explain the difference as the harsh extraction procedures involved had probably removed these labile filaments, readily reduced or lost during preparations and washes in various solutions, including high salt buffers.

Obviously, the assembly of the "nup 153"-like protein into the intranuclear filamentous structures is topogenically restricted and probably nucleated by one or several NPC components representing a "filament-organizing ring." However, it does obviously not require a stoichiometric reaction with a transmembrane anchor or receptor at the NPC rim.

As it has been shown for certain nuclear lamins and NPC

proteins, both the lamina and the NPCs are rapidly disassembled in mitosis, starting at prophase–prometaphase and resulting in distinct mono- or oligomeric subunits. Similar to type A lamins (Gerace et al., 1978; Krohne et al., 1978; Gerace and Blobel, 1980) and several NPC proteins (Davis and Blobel, 1986; Snow et al., 1987; Park et al., 1987; Benavente et al., 1989; Radu et al., 1993) the ~190-kD filament-associated protein is in this stage dispersed throughout most of the central cytoplasm. We suspect that this precisely programmed disassembly and reassembly during mitosis (and meiosis) is affected by protein modification and that the filament subunits are accumulated into the postmitotic nucleus in their soluble form where they then undergo NPC-filament assembly.

The eye-catching organization of the NPC-attached intranuclear filamentous cylinders and their connection to certain intranuclear structures such as nucleoli, invites itself to some apparently irresistible speculations, the most persuasive being a guiding role in nucleocytoplasmic translocation of proteins or ribonucleoproteins, either as channels or by transient entrapment or binding. In this respect, the experiments of Sterne-Marr et al. (1992) are also relevant as their finding of a reduced nuclear import of proteins bearing a "nuclear localization signal" upon depletion of the RL11-binding protein seems also to indicate a contribution of this protein in nuclear uptake of specific proteins.

We thank Sabine Stumpp, Christine Grund, and Arno Floore for competent technical help, Jutta Müller-Osterholt for excellent photographic work, and Dr. Marion Schmidt-Zachmann for valuable discussions.

The study has been supported by the Deutsche Forschungsgemeinschaft.

Received for publication 21 May 1993 and in revised form 29 July 1993.

References

Aaronson, R. P., and G. Blobel. 1975. Isolation of nuclear pore complexes in association with a lamina. *Proc. Natl. Acad. Sci. USA.* 72:1007–1011.

Aebi, U., J. Cohn, L. Buhle, and L. Gerace. 1986. The nuclear lamina is a meshwork of intermediate type filaments. *Nature (Lond.).* 323:560–564.

Aebi, U., M. Häner, J. Troncoso, R. Eichner, and A. Engel. 1988. Unifying principles in intermediate filament (IF) structure and assembly. *Protoplasma.* 145:73–81.

Allen, E. D. 1990. Pores of annulate lamellae and nuclei bind wheat germ agglutinin and monoclonal antibody similarly. *J. Struct. Biol.* 103:140–151.

Bader, B. L., T. M. Magin, M. Freudenmann, S. Stumpp, and W. W. Franke. 1991. Intermediate filaments formed de novo from tail-less cytokeratins in the cytoplasm and in the nucleus. *J. Cell Biol.* 115:1293–1307.

Benavente, R., G. Krohne, R. Stick, and W. W. Franke. 1984. Electron microscopic immunolocalization of a karyoskeletal protein of molecular weight 145,000 in nucleoli and perinuclear bodies of *Xenopus laevis*. *Exp. Cell Res.* 151:224–235.

Benavente, R., M.-C. Dabauvalle, U. Scheer, and N. Chaly. 1989. Functional role of newly formed pore complexes in postmitotic nuclear reorganization. *Chromosoma (Berl.).* 98:233–241.

Blessing, M., U. Rüther, and W. W. Franke. 1993. Ectopic synthesis of epidermal cytokeratins in pancreatic islet cells of transgenic mice interferes with cytoskeletal order and insulin production. *J. Cell Biol.* 120:743–755.

Brasch, K., and Ochs, R. L. 1992. Nuclear bodies (NBs): a newly "rediscovered" organelle. *Exp. Cell Res.* 202:211–223.

Burke, B., J. Tooze, and G. Warren. 1982. A monoclonal antibody which recognizes each of the nuclear lamin polypeptides in mammalian cells. *EMBO (Eur. Mol. Biol. Organ.). J.* 2:361–367.

Cordes, V. C., and G. Krohne. 1993. Sequential O-glycosylation of nuclear pore complex protein gp62 in vitro. *Eur. J. Cell Biol.* 60:185–195.

Cordes, V. C., I. Waizenegger, and G. Krohne. 1991. Nuclear pore complex glycoprotein p62 of *Xenopus laevis* and mouse: cDNA cloning and identification of its glycosylated region. *Eur. J. Cell Biol.* 55:31–47.

Cowin, P., H.-P. Kapprell, W. W. Franke, J. Tamkun, and R. O. Hynes. 1986. Plakoglobin: a protein common to different kinds of intercellular adhering junctions. *Cell.* 46:1063–1073.

Dabauvalle, M.-C., R. Benavante, and N. Chaly. 1988. Monoclonal antibodies to a Mr 68,000 pore complex glycoprotein interfere with nuclear protein uptake in *Xenopus* oocytes. *Chromosoma (Berl.).* 97:193–197.

Dabauvalle, M.-C., K. Loos, and U. Scheer. 1990. Identification of a soluble precursor complex essential for nuclear pore assembly in vitro. *Chromosoma (Berl.).* 100:56–66.

Davidson, E. H. 1986. Gene activity in Early Development. Academic Press, Orlando, FL. 1–670.

Davis, L. I., and G. Blobel. 1986. Identification and characterization of a nuclear pore complex protein. *Cell.* 45:699–709.

Davis, L. I., and G. Blobel. 1987. Nuclear pore complex contains a family of glycoproteins that includes p62: glycosylation through a previously unidentified cellular pathway. *Proc. Natl. Acad. Sci. USA.* 84:7552–7556.

De la Espina, S. M. D., W. W. Franke, G. Krohne, M. F. Trendelenburg, C. Grund, and U. Scheer. 1982. Medusoid fibril bodies: a novel type of nuclear filament of diameter 8 to 12 nm with periodic ultrastructure demonstrated in oocytes of *Xenopus laevis*. *Eur. J. Cell Biol.* 27:141–150.

Eckelt, A., H. Herrmann, and W. W. Franke. 1992. Assembly of a tail-less mutant of the intermediate filament protein vimentin, in vitro and in vivo. *Eur. J. Cell Biol.* 58:319–330.

Fawcett, D. W. 1966. On the occurrence of a fibrous lamina on the inner aspect of the nuclear envelope in certain cells of vertebrates. *Am. J. Anat.* 119:129–146.

Felix, M.-A., J. Pines, T. Hunt, and E. Karsenti. 1989. A post-ribosomal supernatant from activated Xenopus eggs that displays post-translationally regulated oscillation of its $cdc2^+$ mitotic kinase activity. *EMBO (Eur. Mol. Biol. Organ.) J.* 8:3059–3069.

Forbes, D. J. 1992. Structure and function of the nuclear pore complex. *Annu. Rev. Cell Biol.* 8:495–527.

Franke, W. W. 1970. On the universality of nuclear pore complex structure. *Z. Zellforsch.* 105:405–429.

Franke, W. W. 1974. Structure, biochemistry, and functions of the nuclear envelope. *Int. Rev. Cytol.* 39(Suppl.):71–236.

Franke, W. W., and U. Scheer. 1970*a*. The ultrastructure of the nuclear envelope of amphibian oocytes: a reinvestigation. I. The mature oocyte. *J. Ultrastruct. Res.* 30:288–316.

Franke, W. W., and U. Scheer. 1970*b*. The ultrastructure of the nuclear envelope of amphibian oocytes: a reinvestigation. II. The immature oocyte and dynamic aspects. *J. Ultrastruct. Res.* 30:317–327.

Franke, W. W., and P. Reau. 1973. The mitotic apparatus of a zygomycete, *Phycomyces blakesleeanus*. *Arch. Mikrobiol.* 90:323–344.

Franke, W. W., E. Schmid, J. Vandekerckhove, and K. Weber. 1980. A permanently proliferating rat vascular smooth muscle cell with maintained expression of smooth muscle characteristics, including actin of the vascular smooth muscle type. *J. Cell Biol.* 87:594–600.

Franke, W. W., J. A. Kleinschmidt, H. Spring, G. Krohne, C. Grund, M. F. Trendelenburg, M. Stoehr, and U. Scheer. 1981. A nucleolar skeleton of protein filaments demonstrated in amplified nucleoli of *Xenopus laevis*. *J. Cell Biol.* 90:289–299.

Fukui, Y., and H. Katsumaru. 1979. Nuclear actin bundles in *Amoeba*, *Dictyostelium* and human HeLa cells induced by dimethyl sulfoxide. *Exp. Cell Res.* 120:451–455.

Gerace, L., and G. Blobel. 1980. The nuclear envelope lamina is reversibly depolymerized during mitosis. *Cell.* 19:277–287.

Gerace, L., A. Blum, and G. Blobel. 1978. Immunocytochemical localization of the major polypeptides of the nuclear pore complex-lamina fraction. *J. Cell Biol.* 79:546–566.

Gerace, L., Y. Ottaviano, and C. Kondor-Koch. 1982. Identification of a major polypeptide of the nuclear pore complex. *J. Cell Biol.* 95:826–837.

Goldberg, M. W., and T. D. Allen. 1992. High resolution scanning electron microscopy of the nuclear envelope: demonstration of a new, regular, fibrous lattice attached to the baskets of the nucleoplasmic face of the nuclear pores. *J. Cell Biol.* 119:1429–1440.

Holt, G. D., C. M. Snow, A. Senior R. S. Haltiwanger, L. Gerace, and G. W. Hart. 1987. Nuclear pore complex glycoproteins contain cytoplasmically disposed O-linked N-acetylglucosamine. *J. Cell Biol.* 104:1157–1164.

Huegle, B., U. Scheer, and W. W. Franke. 1985. Ribocharin: a nuclear Mr 40,000 protein specific to precursor particles of the large ribosomal subunit. *Cell.* 41:615–627.

Jahn, L., B. Fouquet, K. Rohe, and W. W. Franke. 1987. Cytokeratins in certain endothelial and smooth muscle cells of two taxonomically distant vertebrate species, *Xenopus laevis* and man. *Differentiation.* 36:234–254.

Jarnik, M., and U. Aebi. 1991. Towards a more complete 3 D-structure of the nuclear pore complex. *J. Struct. Biol.* 107:291–308.

Jockusch, B. M., M. Becker, I. Hindennach, and H. Jockusch. 1974. Slime mould actin: homology to vertebrate actin and presence in the nucleus. *Exp. Cell Biol.* 89:141–146.

Kartenbeck, J., K. Schwechheimer, R. Moll, and W. W. Franke. 1984. Attachment of vimentin filaments to desmosomal plaques in human meningioma cells and arachnoidal tissue. *J. Cell Biol.* 98:1072–1081.

Kessel, R. G. 1983. The structure and function of annulate lamellae: porous cytoplasmic and intranuclear membranes. *Int. Rev. Cytol.* 82:181–303.

Krohne, G., W. W. Franke, S. Ely, A. D'Arcy, and E. Jost. 1978*a*. Localization of a nuclear envelope-associated protein by indirect immunofluorescence microscopy using antibodies against a major polypeptide from rat liver fractions enriched in nuclear envelope-associated material. *Cytobiologie.*

18:22–38.
Krohne, G., and W. W. Franke. 1983. Proteins of pore complex lamina structures from nuclei and nuclear membranes. *Methods Enzymol.* 96:597–608.
Krohne, G., W. W. Franke, and U. Scheer. 1978*b*. The major polypeptides of the nuclear pore complex. *Exp. Cell Res.* 116:85–102.
Krohne, G., R. Stick, J. A. Kleinschmidt, R. Moll, W. W. Franke, and P. Hausen. 1982. Immunological localization of a major karyoskeletal protein in nucleoli of oocytes and erythrocytes of *Xenopus laevis*. *J. Cell Biol.* 94:749–754.
Kubai, D. F. 1975. The evolution of the mitotic spindle. *Int. Rev. Cytol.* 43:167–227.
Laemmli, U. K. 1970. Cleavage of structural proteins during the assembly of the head of bacteriophage T4. *Nature (Lond.).* 227:680–685.
Maul, G. G. 1977. The nuclear and cytoplasmic pore complex. Structure, dynamics, distribution, and evolution. *Int. Rev. Cytol.* 6:75–186.
Nehrbass, U., H. Kern, A. Mutvei, H. Horstmann, B. Marshallsey, and E. C. Hurt. 1990. NSP1: a yeast nuclear envelope protein localized at the nuclear pores exerts its essential function by its carboxyterminal domain. *Cell.* 61:979–989.
O'Farrell, P. Z., H. M. Goodman, and P. H. O'Farrell. 1977. High resolution two-dimensional gel electrophoresis of basic as well as acidic proteins. *Cell.* 12:1133–1142.
Osborn, M., and K. Weber. 1980. Dimethylsulfoxide and the ionophore A23187 affect the arrangement of actin and induce nuclear actin paracrystals in PtK2 cells. *Exp. Cell Res.* 129:103–114.
Park, M. K., M. D'Onofrio, M. C. Willingham, and J. A. Hanover. 1987. A monoclonal antibody against a family of nuclear pore proteins (nucleoporins): O-linked N-acetylglucosamine is part of the immunodeterminant. *Proc. Natl. Acad. Sci. USA.* 84:6462–6466.
Radu, A., G. Blobel, and R. W. Wozniak. 1993. Nup155 is a novel nuclear pore complex protein that contains neither repetitive sequence motifs nor reacts with WGA. *J. Cell Biol.* 121:1–9.
Ris, H. 1989. Three-dimensional imaging of cell ultrastructure with high resolution low voltage SEM. *Inst. Phys. Conf. Ser.* 98:657–662.
Ris. H. 1991. The three dimensional structure of the nuclear pore complex as seen by high voltage electron microscopy and high resolution low voltage scanning electron microscopy. *EMSA Bull.* 21:54–56.
Scheer, U., J. Kartenbeck, M. F. Trendelenburg, J. Stadler, and W. W. Franke. 1976*a*. Experimental disintegration of the nuclear envelope. Evidence for pore-connecting fibrils. *J. Cell Biol.* 69:1–18.
Scheer, U., M. F. Trendelenburg, and W. W. Franke. 1976*b*. Regulation of transcription of genes of ribosomal RNA during amphibian oogenesis. *J. Cell Biol.* 69:465–489.
Scheer, U., M.-C. Dabauvalle, H. Merkert, and R. Benavente. 1988. The nuclear envelope and the organization of the pore complexes. *Cell. Biol. Int. Rep.* 12:669–689.
Snow, C. M., A. Senior, and L. Gerace. 1987. Monoclonal antibodies identify a group of nuclear pore glycoproteins. *J. Cell Biol.* 104:1143–1156.
Sterne-Marr, R., J. M. Blevitt, and L. Gerace. 1992. O-linked glycoproteins of the nuclear pore complex interact with a cytosolic factor required for nuclear protein import. *J. Cell Biol.* 116:271–280.
Stuurman, N., A. de Graaf, A. Floore, A. Josso, B. Humbel, L. de Jong, and R. van Driel. 1992. A monoclonal antibody recognizing nuclear matrix-associated nuclear bodies. *J. Cell Sci.* 101:773–784.
Sukegawa, J., and G. Blobel. 1993. A nuclear pore complex protein that contains zinc finger binding motifs, binds DNA, and faces the nucleoplasm. *Cell.* 72:29–38.
Thomas, J. O., and R. D. Kornberg. 1975. An octamer of histones in chromatin and free in solution. *Proc. Natl. Acad. Sci. USA.* 72:2626–2630.
Trendelenburg, M. F., and R. G. McKinnell. 1979. Transcriptionally active and inactive regions of nucleolar chromatin in amplified nucleoli of fully grown oocytes of hibernating frogs, *Rana pipiens* (Amphibia, Anura). *Differentiation.* 15:73–95.
Wilken, N., U. Kossner, J.-L. Senécal, U. Scheer, and M.-C. Dabauvalle. 1993. Nup180, a novel nuclear pore complex protein localizing to the cytoplasmic ring and associated fibrils. *J. Cell Biol.* 1345–1354.